Journal of Thermal Analysis, Vol. 38 (1992) 2417-2436

THERMAL DEHYDRATION AND DECOMPOSITION OF NICKEL CHLORIDE HYDRATE ($NiCl_2 \cdot xH_2O$)

*S. K. Mishra and S. B. Kanungo**

REGIONAL RESEARCH LABORATORY, BHUBANESWAR-751013, INDIA

(Received August 12, 1991)

The dehydration and decomposition characteristics of an undried and a partly dried sample of $NiCl_2 \cdot xH_2O$ have been investigated by isothermal and non-isothermal (TG and DTA) methods in static air as well as flowing nitrogen environment. While the isothermal weight loss method fails to distinguish between different steps of reaction, TG curves upto 800°C reveal as many as five steps in static air and four steps in nitrogen atmosphere. However, both methods indicate that $NiCl_2$ is stable upto 400°C above which dehydrochlorination takes place in presence of water vapour. The intermediate products of dehydration and decomposition at different temperatures have been characterized by chemical analysis, X-ray diffraction, infrared and diffuse reflectance spectroscopy. All these methods reveal the presence of water in samples calcined at even 400°–600°C. Thermodynamic functions for different steps of dehydration have been calculated and discussed in the light of the possible structural changes occurring in the partially dehydrated products.

Keywords: mechanism of dehydration, $NiCl_2 \cdot xH_2O$, thermodynamic parameters

Introduction

Selective chlorination and chloridization are two important methods used in the extraction of metals from their ores. The desired selectivity is usually achieved by utilizing the differential thermal stability of metal chlorides. This principle has been applied in the extraction of trace metals such as Ni, Cu, Co, Zn, etc. from sea-bed manganese module [1–3] or Ni and Co from lateritic iron ore [4–6] whereby the poorly stable iron chloride is decomposed at a suitable temperature without seriously affecting the

* Author to whom correspondence should be addressed

John Wiley & Sons, Limited, Chichester
Akadémiai Kiadó, Budapest

chlorides of trace metals which are subsequently leached out in water. One important advantage of chloridizing roasting is that the thermal decomposition of many hydrated chlorides produce gaseous hydrogen chloride which can be recycled in the process. Though the principle of pyrohydrolysis has been widely used [7–9] in the separation of iron, magnesium etc. little information is available on the thermal decomposition behaviour of many metal chlorides particularly in their hydrated forms.

Literature survey reveals that though some work has been carried out on the thermal deaquation of hydrated chlorides of Ba, Mg and Co [10–17], very little work has been reported on the thermal decomposition (including dechlorination) of hydrated chlorides of many important base metals. The present investigation was therefore undertaken to gain further understanding not only on the thermal deaquation of some important metal chlorides, but also on the decomposition of dehydrated or partially dehydrated metal chlorides. In this paper we report the results of investigation on $NiCl_2 \cdot xH_2O$.

Experimental

Materials

An undried reagent grade (BDH, India) hydrated nickel chloride and a partly dried sample were used in the present investigation. The latter was prepared by drying the former sample over concentrated sulphuric acid and phosphorus pentoxide for a period of 8 days. Both thermogravimetric and chemical analyses reveal that undried and dried samples contain 7.55 and 5.53 moles of water of hydration respectively.

Methods

Isothermal decomposition

Isothermal decomposition of $NiCl_2 \cdot 7.55H_2O$ was carried out by heating 1 g of sample in batches in a laboratory muffle furnace of chamber size 10 cm×30 cm. Finely ground samples were taken in a series of silica crucibles and introduced in the furnace at the desired temperature which was maintained at ±5°C at a temperature below 400°C and ±8°C at a temperature in the range of 400°–600°C. The zero time ($t = 0$) begins from the moment each crucible containing the sample was introduced in the furnace. After heating for a requisite period of time, the sample was withdrawn from the furnace, cooled in a desiccator over silica gel and weighed.

TG and DTA

Thermogravimetric (TG) and differential thermal analysis (DTA) were carried out in a Netzsch (model STA-409) thermoanalyzer at a heating rate of 10 deg·min^{-1} using Pt-crucible and α-Al_2O_3 as reference material. Experiments were carried out under both static air (self-generated atmosphere) and flowing nitrogen (50 ml/min) environments. Heats of different steps of dehydration reaction were estimated by taking the ther-

mograms of various substances with known heats of physical-chemical changes (kJ/g) were plotted against their corresponding DTA peak areas (cm^2/g). The samples were known from the list provided by Wendlandt [18] and the DTA peak areas were measured by graphical method.

X-ray diffraction

X-ray diffraction patterns of the products of decomposition were taken in a Philips Diffractometer using Cu-K_α radiation.

Infrared spectra

FT-IR spectra of some intermediate products of decomposition were taken in a Nicolet IR spectrophotometer using KBr pellet technique. The pellets were dried at 250°C for 1 h before taking the spectra.

Diffuse reflectance spectra (DRS)

DRS of original $NiCl_2 \cdot xH_2O$ and its decomposition products at 100°, 200° and 400°C were taken in a Varian UV-VIS spectrophotometer fitted with a double-beam reflectance attachment. Finely ground samples were compressed in a Herzog (Germany) compressing machine against two types of white background material namely, magnesium carbonate and boric acid (E. Merc, India). The finely ground samples were placed in such a way that they occupied the central region of the compressed discs of 30 mm dia and 4 mm thickness. Two separate discs of only blank materials were also made for calibrating the instrument for 100% reflectance. No difference in the spectra was observed when both boric acid and $MgCO_3$ were used as background materials.

Chemical analysis

Chemical analysis of the products obtained at different temperatures was carried out by dissolving the sample in dilute HNO_3 and estimating nickel and chloride by titration with standard EDTA and $AgNO_3$ solution respectively.

In order to characterize further the products of decomposition at temperatures above 270°C, the water insoluble fractions were separated by leaching in water at 70°–80°C and filtering through dry G4 sintered glass crucibles. After thorough drying at 150°C, the amounts of insoluble fractions were determined from the differences in the weights of the crucibles. The insoluble fractions were dissolved in hot dilute HNO_3 and analysed for total Ni as above.

Results and discussion

Isothermal decomposition

Figure 1 depicts the isothermal weight loss curves at various temperatures. All the data presented in the figure are the averages of duplicate and in some cases triplicate

measurements. While at lower temperatures (100°–200°C) the deviations were within ±4%, at temperatures above 200°C nearly consistent (±1.0%) values were obtained. Unlike other temperatures the rate of dehydration at 100°C is almost linear upto 60 minutes where the total weight loss (about 32%) is the same as the observed one at 150°C. This corresponds to about 4.7 moles of water, indicating that this quantity of water initially undergoes melting and subsequently dehydrates upto 150°C. The linear behaviour for 100°C is probably due to the fact that the rate of evaporation of water from a constant surface area (sample holder) is zero order and is therefore, independent of reaction mechanism [14]. The figure further shows that the rate of weight loss sharply increases as the temperature is increased above 200°C. At 270° and 400°C a maximum weight loss of about 50% is reached within 30 min corresponding to the loss of about 7.5 moles of water. At 500°–600°C weight loss curves show further increase and the process continues even after 60 min suggesting that in addition to dehydration decomposition of $NiCl_2$ also takes place. At 600°C the total weight loss after 60 minutes of heating is about 70% against the maximum loss of about, 73.3% found after calcination at 800°C for 1 h.

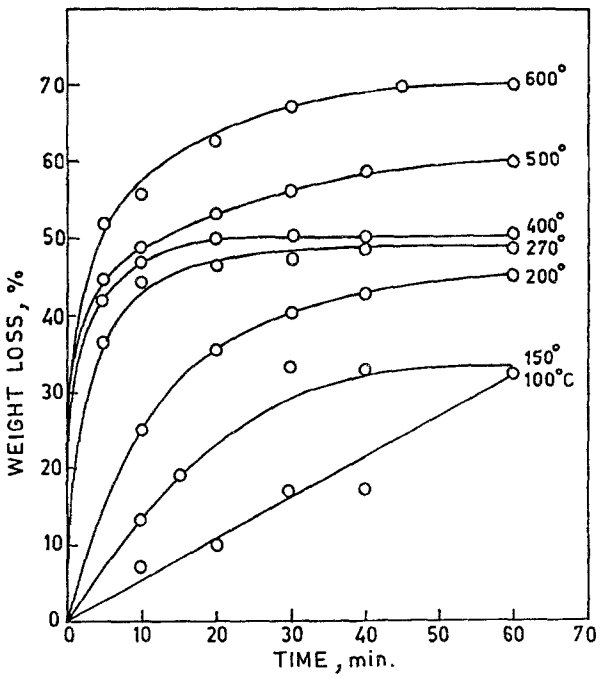

Fig. 1 Isothermal decomposition of $NiCl_2 \cdot 7.55H_2O$ in air

DTA and TG

Figures 2 and 3 illustrate DTA and TG traces of the two samples in static air and flowing nitrogen environment respectively. Let us first consider the thermogram of the

undried sample. Under the former condition while five endothermic peaks are observed from ambient to 300°C only four endothermic peaks can be observed in nitrogen atmosphere. The first peak due to melting of a certain portion of water of hydration shifts from 60°C under static air to 80°C, in nitrogen atmosphere wherein the second endo peak for the loss of 1 mole of water at 100°C does not appear. This is supported from the TG curve which shows that the two stage water loss in static air changes to single stage loss in nitrogen atmosphere in the temperature range of 80°–160°C. In the self-generated atmosphere of H_2O vapour dehydration takes place little earlier than the phase transition (to lower hydrate), whereas in flowing nitrogen environment both the processes take place almost simultaneously. This phenomenon is usually observed in the thermal dehydration of many $MCl_2 \cdot 6H_2O$ which shows incongruent melting.

The other three endothermic effects upto 300°C occur not only at the same temperatures (160°, 200° and 280°C) in both the atmospheres, but also their natures are similar and correspond well with the different stages of weight losses in TG curves. In static air the successive losses of water molecules at 100°, 160°, 200° and 280°C are 1.0, 4.35, 1.0 and 1.0 respectively. On the other hand, in nitrogen atmosphere the corresponding losses are 4.55, 1.0 and 1.4 molecules respectively (Table 1). Above 400°C TG curves in

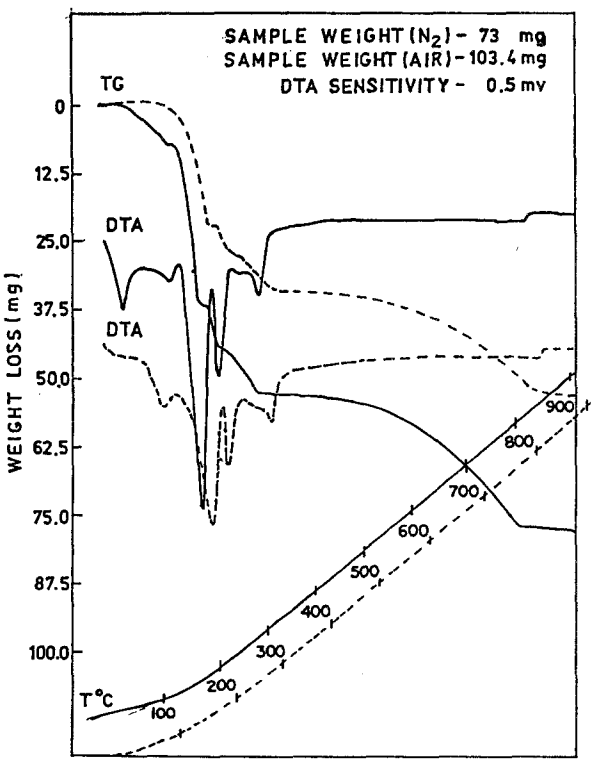

Fig. 2 Thermal curves of $NiCl_2 \cdot 7.55H_2O$. Solid line represents static air and broken line represents flowing nitrogen environments

both cases exhibit gradual loss in weight and attains a complete plateau region at 800°C. The decomposition in the temperature range of 300°–800°C involves complex processes of dehydrochlorination and dechlorination. Table 1 suggests that the observed weight losses at 820°C agree well with those calculated from the proposed reactions involving dehydrochlorination, dechlorination and partial oxidation.

The thermal analysis of partly dried nickel chloride hydrate ($NiCl_2 \cdot 5.53H_2O$) exhibits some features (Fig. 3) which are distinctly different from those of undried sample. First, unlike undried sample only a fewer moles of water of crystallization undergo melting at relatively lower temperature (40°–45°C). No loss of water takes place during melting. However a DTA shoulder at 110°C indicates a small initial loss of about 5% water followed by a sharp loss in weight upto 160°–170°C. Secondly, the melting of monohydrate salt at 230°–240°C can be rather distinctly identified before the loss of last mole of water to form anhydrous salt as indicated by weight loss in TG curve (Table 2). Thirdly, DTA exhibits an endothermic effect in the temperature range of 860°–930°C for the decomposition of apparently anhydrous salt, a process which is more complicated than the decomposition of monohydrated salt for undried sample (Table 1). Probably, the anhydrous salt adsorbs one mole of water vapour from ambient atmosphere to undergo rapid hydrolysis. In order to clarify this aspect evolved gas analysis has been undertaken, the results of which will be communicated in due course.

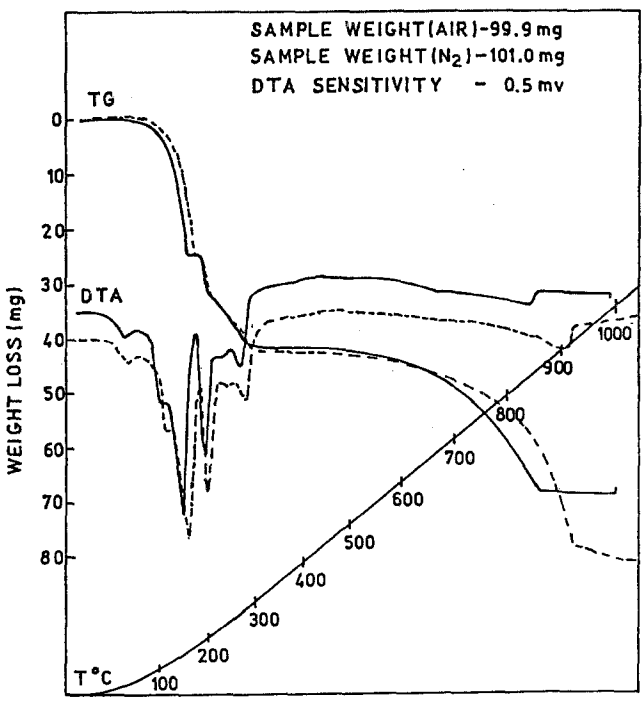

Fig. 3 Thermal curves of $NiCl_2 \cdot 5.53H_2O$. Solid line represents static air and broken line represents flowing nitrogen environments

Table 1 Calculated and observed weight losses for different proposed steps of dehydration and decomposition of $NiCl_2 \cdot 7.55H_2O$ in air and flowing nitrogen

No.	Temp./ °C	Proposed steps (Reactions)	Cumulative weight loss/%			
			In static air		In flowing N_2	
			Calcd.	Obsd.	Calcd.	Obsd.
1	110	$NiCl_2 \cdot 7.55H_2O(s) \rightarrow NiCl_2 \cdot 6.55H_2O(l) + H_2O(g)$	6.78	6.65	–	–
2	160	$NiCl_2 \cdot 6.55H_2O(l) \rightarrow NiCl_2 \cdot 2.2H_2O(s) + 4.35H_2O(g)$	36.28	35.56	–	–
		$NiCl_2 \cdot 7.55H_2O(l) \rightarrow NiCl_2 \cdot 3.0H_2O(s) + 4.55H_2O(g)$	–	–	30.84	30.70
3	200	$NiCl_2 \cdot 2.2H_2O(s) \rightarrow NiCl_2 \cdot 1.2H_2O(s) + H_2O(g)$	43.04	43.04	–	–
		$NiCl_2 \cdot 3H_2O(s) \rightarrow NiCl_2 \cdot 2H_2O + H_2O(g)$	–	–	37.62	37.52
4	280	$NiCl_2 \cdot 1.2H_2O(s) \rightarrow NiCl_2 \cdot 0.2H_2O(s) + H_2O(g)$	49.82	50.80	–	–
		$NiCl_2 \cdot 2H_2O(s) \rightarrow NiCl_2 \cdot 0.6H_2O(s) + 1.4H_2O(g)$	–	–	46.90	47.12
5	820	$NiCl_2 \cdot 0.2H_2O(s) + 0.4O_2(g) \rightarrow NiO(s) + 0.4HCl(g) + 1.6Cl(g)$	75.42	75.00	–	–
		$NiCl_2 \cdot 0.6H_2O(s) + 0.2O_2(g) \rightarrow NiO(s) + 1.2HCl(g) + 0.8Cl(g)$	–	–	73.40	73.30

Table 2 Calculated and observed weight losses for different proposed steps of dehydration of $NiCl_2 \cdot 5.53H_2O$ in air and flowing nitrogen

No.	Temp./ °C	Proposed steps (Reactions)	Cumulative weight loss/%			
			In static air		In flowing N_2	
			Calcd.	Obsd.	Calcd.	Obsd.
1	40	$NiCl_2 \cdot 5.53H_2O \rightarrow$ In congruent melting in 2-3 moles of water of crystallization	–	–	–	–
2	145	$NiCl_2 \cdot 5.53H_2O \rightarrow NiCl_2 \cdot 2.33H_2O(s) + 3.20H_2O(v)$	25.12	25.05	25.12	25.2
3	190	$NiCl_2 \cdot 2.33H_2O(s) \rightarrow NiCl_2 \cdot 1.33H_2O(s) + H_2O(v)$	32.97	33.04	33.0	33.17
4	270	$NiCl_2 \cdot 1.33H_2O(s) \rightarrow NiCl_2(s) + 1.33H_2O(l)$				
		$1.33H_2O(l) \rightarrow 1.33H_2O(v)$	43.18	42.54	43.18	42.60

Physico-chemical characterization of the products of decomposition at different temperatures

Chemical analysis

Table 3 depicts the chemical analysis of the products obtained after 1 h of heating at different temperatures along with the weight losses observed by both the methods of heating. The results indicate that no appreciable loss of chlorine takes place upto 400°C. Moreover, at this temperature both isothermal and non-isothermal heating in static air exhibit an average weight loss of about 51.4% against the calculated loss of about 51.3% for 7.55 moles of water. Chemical analysis shows that at 500°C there is only a small loss of chlorine, whereas at 600°C Cl/Ni ratio is about unity indicating the formation of either hydroxychloride (Ni(OH)Cl) or oxychloride (Ni_2–O–Cl_2). Further identification was therefore carried out by other physical methods such as XRD and infrared spectra. At 850°C the nickel content of the product is about 74.7% which is about 3.9% less than the calculated quantity for pure NiO. Such cation deficiency is not uncommon for a p-type semiconductor like NiO.

Table 3 Chemical analysis of the intermediate products of decomposition of $NiCl_2 \cdot 7.55H_2O$ at different temperatures (Period of heating 1 h). Observed weight losses are also given

Temp./	Total Ni	Total Cl	Cl/Ni	Weight loss, %	
°C	%	%	Mole ratio	Isothermal	Non-isothermal
150	32.19	43.57	2.24:1	32.5	29.8
200	41.05	50.14	2.02:1	45.0	43.0
270	41.57	51.07	2.03:1	48.3	47.1
400	41.75	51.00	2.02:1	51.4	51.5
500	44.71	45.88	1.70:1	60.0	52.8
600	45.80	30.18	1.09:1	70.0	56.6
700	53.73	21.00	0.65:1	71.0	64.0
820	74.70	–	–	–	–

Table 4 Chemical analysis of water soluble and insoluble fractions of the products of decomposition at different temperatures (period of calcination 1 h)

Temp./	Soluble fraction				Insoluble fraction	
°C	weight/	Ni	Cl	Cl/Ni	weight/	Ni
	%	%	%	Mole ratio	%	%
400	97.1	34.36	45.68	2.20:1	2.9	60.94
500	88.2	41.63	52.02	2.07:1	11.8	67.74
600	60.4	35.28	44.17	2.07:1	39.6	73.70
700	48.5	29.10	43.30	2.03:1	51.5	77.00

In order to get further information on the chemical composition of the intermediate product of decomposition a known quantity of it was leached in hot water for 30 min. It was observed that the entire product of thermolysis upto 270°C is soluble in water suggesting the presence of only $NiCl_2$. Data in Table 4 indicate that insoluble product begins to form at 400°C although its quantity is very small upto 500°C. At 600°C the amount of insoluble fraction increases to 39.6% and at 850°C the entire product is insoluble in water. Assuming that at 600°C soluble and insoluble fraction consist of $NiCl_2$ and $Ni(OH)_2$ respectively their corresponding mole ratio is 1.09. Similar assumption for 700°C leads to a ratio of 0.67. In both cases they agree well with the Cl/Ni ratio as found from total analysis of the products (Table 3).

X-ray diffraction

Figure 4 illustrates the diffractograms of various intermediate products of decomposition. The figure also gives the standard patterns of partially dehydrated and anhydrous $NiCl_2$, hydroxychloride for ready reference. It can be seen that the products of decomposition at 150° and 270°C are heterogeneous mixtures of $NiCl_2 \cdot 4H_2O$, $NiCl_2 \cdot 2H_2O$ and some basic chloride indicating that some loss of chlorine takes place at temperature above 250°C. At 400° and 500°C of calcination the major phases are

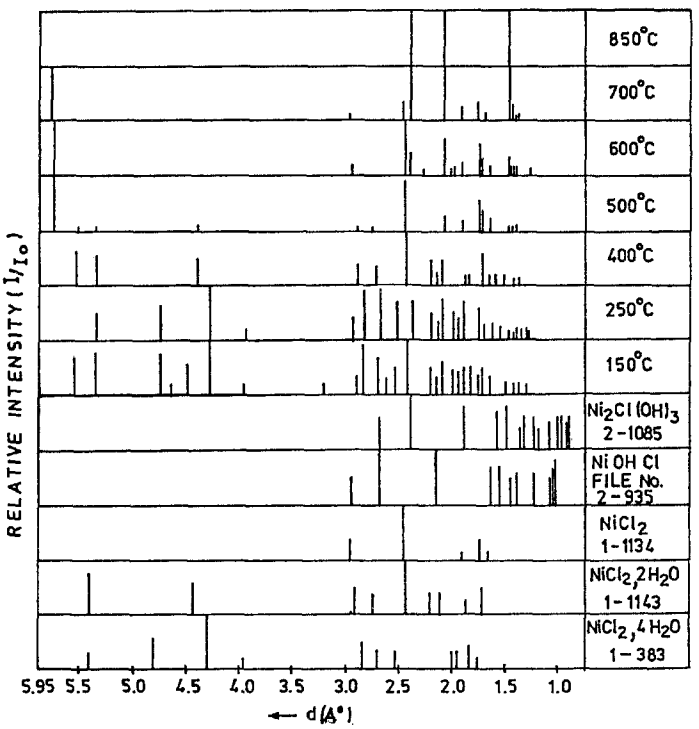

Fig. 4 X-ray diffraction pattern on $NiCl_2 \cdot 7.55H_2O$ calcined at different temperatures for one hour. Standard diffractograms of possible intermediates are also included for reference

$NiCl_2 \cdot 2H_2O$ and anhydrous $NiCl_2$ respectively. At 600°C the formation of NiO begins but a number of additional lines also appear which can be identified with Ni(OH)Cl and $Ni_2Cl(OH)_2$. At 700°C NiO is the major phase with small quantity of anhydrous $NiCl_2$. At 850°C the only phase identified is of NiO.

Infrared spectra

The main difficulty in obtaining the true infrared spectrum of a metal chloride in an alkali halide matrix is the possible interaction or exchange of halide ions between the matrix and the probe. This may happen not only during grinding with alkali halide but also during pellet formation under high pressure. While the exchange of halide ions does not alter the vibration of O–H groups, the formation of solid solution gives rise to a bending vibration of H_2O around 1640 cm^{-1} even for a calcined sample [17].

The spectra of thermally treated samples are very broad in the range of 4000–3000 cm^{-1}, thereby making it difficult to interpret O–H stretching vibration. It is observed that the O–H vibration due to the presence of hydrolysed product is discernible only at 400°–500°C. However, the absorption band around 1640 cm^{-1} become sharper as the temperature of calcination is increased from 250° to 600°C suggesting the possible interaction of KBr with $NiCl_2 \cdot H_2O$ [17]. In order to get further insight into the nature of occurrence of free and structural OH groups FT-IR spectra were taken for 500° and 600°C calcined samples as illustrated in Fig. 5 which suggests that for 500°C cal-

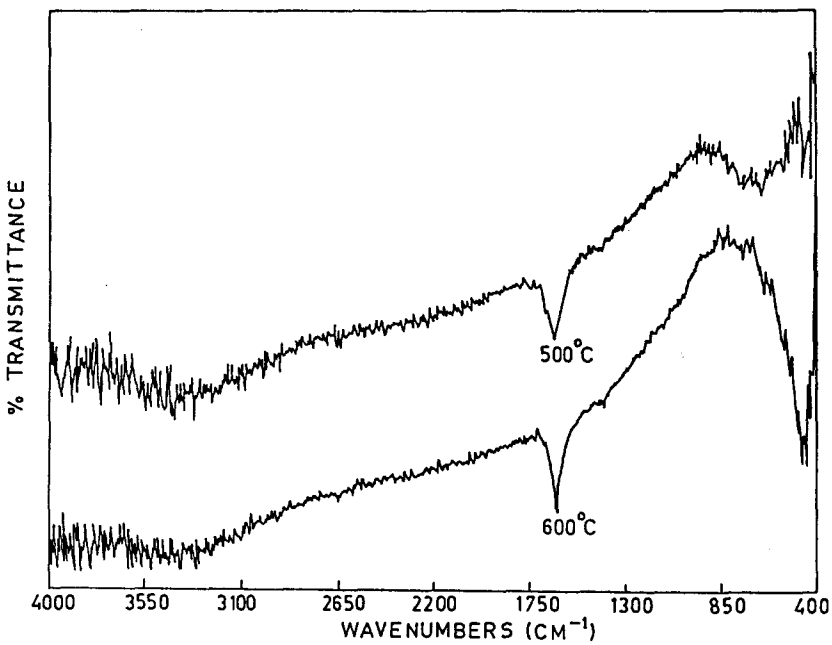

Fig. 5 FT-IR spectra of $NiCl_2 \cdot 7.55H_2O$ calcined at 500° and 600°C

cined sample there are more than one type of OH group having different bond lengths. This indicates that thermal hydrolysis of $NiCl_2$ hydrate yields different products having different Cl/OH mole ratios. While the bands at 746 cm^{-1} and 660 cm^{-1} represent the bending vibration or libration of Cl–Ni–OH, the poorly defined band at 470 cm^{-1} indicate NiO lattice vibration. At 600°C the bending vibration of Cl–Ni–OH fades out considerably and lattice vibration of NiO becomes the most predominant feature of the spectrum.

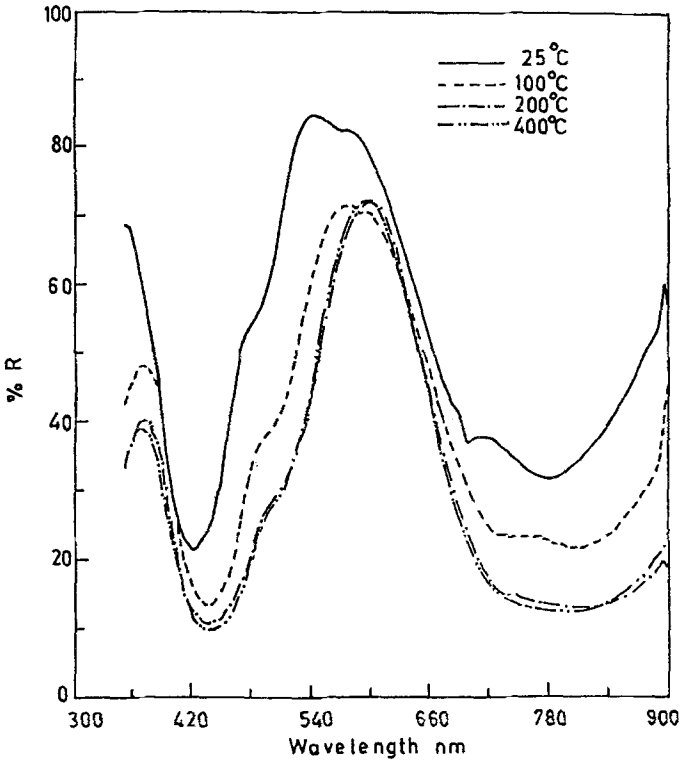

Fig. 6 Diffuse reflectance spectra of $NiCl_2 \cdot 7.55H_2O$ calcined at different temperatures using boric acid as standard

Diffuse reflectance spectra

Diffuse reflectance spectra of $NiCl_2 \cdot xH_2O$ and its calcined products are shown in Fig. 6. Although some of the important transitions could not be observed in the range of wavelength scanned, the occurrence of a few minima in the spectra provide some useful information on the structures of dehydrated products. Table 5 shows that for $NiCl_2 \cdot xH_2O$ at least five minima are observed in accordance with weak field d^8 electrons. Out of these four could be identified for electronic transitions, whereas the shoulder at 480 nm is due to spin-orbit coupling and is present in all the samples. The

disappearance of two weak spin-forbidden transitions, $^1E_g \leftarrow {}^3A_{2g}$ at 100°C and $^1T_{2g} \leftarrow {}^3A_{2g}$ at 200°C suggests that the compound transforms to weakfield as chlorine gradually occupies the coordination sphere Ni^{2+}. At 400°C only two very strong transitions persist from which the ligand field parameters are obtained as follows:

$$^3T_{1g}\ (F) \leftarrow {}^3A_{2g} = 18\ Dq \quad (1)$$

$$^3T_{1g}\ (P) \leftarrow {}^3A_{2g} = 15\ B + Dq \quad (2)$$

Table 5 shows that Dq and consequently crystal field stabilization energy (cf.Se. = 12 Dq) gradually decrease with loss of water upto 200°C. Since anhydrous $NiCl_2$ adsorbs moisture even during experiment Dq value increases slightly. However, low Dq values in all cases indicate tetragonal distortion.

Table 5 Minima in diffuse reflectance spectra and the ligand field parameters for $NiCl_2 \cdot xH_2O$ and its intermediate products of dehydration

Wavelength/nm				Assignments of minima (transitions)
$NiCl_2 \cdot xH_2O$ /	Calcination temperatures/°C			
nm	100	200	400	
718.0	807.7	819.8	801.1	$^3T_{1g} \leftarrow {}^3A_{2g}$
699.5	–	–	–	$^1E_g \leftarrow {}^3A_{2g}$
567.2	592.5	–	–	$^1T_{1g} \leftarrow {}^3A_{2g}$
480.0	490.0	500.6	502.5	Spin-Orbit Coupling
418.9	434.9	436.3	436.3	$^3T_{1g}^{(P)} \leftarrow {}^3A_{2g}$
		Ligand field parameters		
711.3	687.8	677.7	693.4	Dq (cm^{-1})
1022.4	982.6	985.8	973.3	B (cm^{-1})
0.696	0.700	0.687	0.712	Dq/B
8535.6	8253.6	8132.4	8320.8	C.f.s.e. (cm^{-1})

Thermodynamics of dehydration

In order to derive thermodynamic parameters for various steps of dehydration and decomposition, it is essential to know ΔH_f°, S_f° and C_p values of both the initial and final products as well as the intermediate products of reaction. Though ΔH_f° and S_f° values of some well-defined hydrates of $NiCl_2$ and anhydrous salt at 298 K are available in literature [18], the initial and intermediate products of dehydration in the present work do not correspond to those reported in the literature and as such cannot be used in the present calculation. Therefore, to derive the thermodynamic data for the dehydration of $NiCl_2$

hydrate, we have adopted an approach similar to that used by Grindstaff and Fogel [19] for dehydration of $CoCl_2 \cdot 6H_2O$.

The loss of m moles of water during dehydration of $NiCl_2 \cdot nH_2O$ can be written as

$$NiCl_2 \cdot nH_2O\ (s) \rightarrow NiCl_2 \cdot (n\text{-}m)H_2O\ (s) + mH_2O\ (v)$$

After making an extensive survey of the literature values of enthalpy and entropy changes of a large number of hydrated salts, Gringstaff and Fogel [19] have observed that the average values of ΔH reac. and ΔS reac. for the loss of one mole of water are -55.2 kJ and $150.4\ JK^{-1}$ respectively. These values are close to the sublimation of water vapour from ice-like structure. This observation helps in calculating the enthalpy and entropy of dehydration without any prior knowledge of the heat of formation of the intermediate products of dehydration assuming that change in heat capacity is negligibly small. For the loss of $(n-m)$ moles of water we have

$$\Delta H^{\circ}_{reac} = -(n-m)\ 55.2\,kJ \tag{3}$$

$$\Delta S^{\circ}_{reac} = (n-m)\ 150.4\,J \cdot mol^{-1} \cdot K^{-1} \tag{4}$$

While the above relationships are valid for dehydration from crystalline phase, the same may not be true when a part of the water of hydration loses its ice-like bonding after getting melted incongruently. In such a case the dehydration probably takes place by simple evaporation of liquid water from the molten phase with latent heat of evaporation of about $41.1\ kJ \cdot mol^{-1}$. As such evaporation takes place at temperature higher than 100°C the value of the heat of evaporation may differ from $41.1\ kJ \cdot mol^{-1}$. Table 6 indicates that for $NiCl_2 \cdot 7.55H_2O$ experimental values of heat of dehydration agrees well within experimental error with those calculated on the basis of evaporation of water.

In the case of $NiCl_2 \cdot 5.53H_2O$ (Table 6B) no extensive melting takes place (roughly 2 moles of water assuming latent heat of melting of ice as $6\ kJ \cdot mol^{-1}$). The ice structure of crystal hydrate is not basically disturbed upto the loss of 4.20 moles of water. However, the appearance of small endothermic effect just before the loss of last mole of water suggests the second stage of melting of lone water molecule which eventually evaporates as free water. The calculated entropy changes for all these stages agree well with those found on the basis of evaporation from either ice-like structure or from free-water.

Thermochemistry of nickel chloride hydrates

Although in the present work the values of n and m of the intermediate products of dehydration are found to be fractional numbers, it is worthwhile to present thermochemical data of mono, di, tetra and hexahydrate of $NiCl_2$ for which no detailed studies have been carried out so far. The heats of formation of different hydrates of

Table 6 Thermodynamic data of the dehydration of hydrate nickel chloride in air and flowing nitrogen environments

A. Dehydration of $NiCl_2 \cdot 7.55H_2O$

Environment	DTA peak temp./K	Melting or number of mols of H_2O lost	$\Delta H^{\circ}_{Reac} \pm 15$ kJ·mol^{-1}		$\Delta S^{\circ}_{Reac} \pm 20$ J·mol^{-1}K^{-1}		$\Delta G^{\circ(g)}_T$ at peak temp./ kJ·mol^{-1}
			Calcd.	Found[c]	Calcd.	Found[f]	
Air	333	Melting	–	48.0	–	–	–
N_2	353	Melting	–	55.8	–	–	–
Air	433	4.35	178.8[a]	201.8	479.4[d]	532.8	28.9
N_2	433	4.55	187.0[a]	219.5	501.4[d]	576.4	30.1
Air	473	1.20	49.3[a]	51.4	132.2[d]	136.6	13.2
N_2	473	1.00	41.1[a]	40.5	110.2[d]	108.9	11.0
Air	553	1.00	41.1[a]	38.5	110.2[d]	105.4	19.8
N_2	553	1.40	57.4[a]	48.6	154.3[d]	138.0	27.8

Table 6 Continued

B. Dehydration of $NiCl_2 \cdot 5.53H_2O$

Environment	DTA peak temp./K	Melting or number of mols of H_2O lost	$\Delta H^{\circ}_{Reac} \pm 15$ kJ·mol^{-1}		$\Delta S^{\circ}_{Reac} \pm 20$ J·mol^{-1}K^{-1}		$\Delta G^{\circ g)}_{T}$ at peak temp./ kJ·mol^{-1}
			Calcd.	Found[c)]	Calcd.	Found[f)]	
Air	318	Melting	–	12.5	–	–	–
N_2	313	Melting	–	13.0	–	–	–
Air	418	3.2	176.6[b)]	182.0	481.3[e)]	494.0	24.6
N_2	423	3.2	176.6[b)]	200.0	481.3[e)]	536.6	27.0
Air	463	1.0	55.2[b)]	65.0	150.4[e)]	171.7	14.5
N_2	463	1.0	55.2[b)]	61.0	150.4[e)]	163.1	14.5
Air	543	1.33	54.6[a)]	40.0	146.6[d)]	101.3	15.0
N_2	543	1.33	54.6[a)]	38.0	146.6[d)]	97.6	15.5

[a)] Calculated on the basis of 41.1 kJ·mol^{-1} as latent heat of evaporation of water at 373 K

[b)] Calculated on the basis of 55.2 kJ·mol^{-1} as the heat of sublimation of water from ice-like structure at 298 K.

[c)] Obtained from area under DTA peak.

[d)] Calculated on the basis of 110.2 J·mol^{-1}K^{-1} as entropy of evaporation of water.

[e)] Calculated on the basis of 150.4 J·mol^{-1}K^{-1} as entropy of sublimation from ice-like structure.

[f)] Calculated by using the values of ΔH° and ΔG_T in columns (5) and (8) respectively.

[g)] Calculated by using the values of ΔH° and ΔS° in columns (4) and (8) respectively.

Table 7 Thermochemical data of the different hydrates of nickel chloride in their crystalline forms

Crystalline compounds	$-\Delta H^{\circ}_{f(n)}$ / kJ·mol^{-1}		$S^{\circ}_{f(n)}$ / J·mol^{-1}K^{-1}		Lattice energies $U_{1(n)}$ /kJ·mol^{-1}		$-\Delta H_w / n$ kJ·mol^{-1}
	(Ref. 18)	Calcd.*	(Ref. 8)	Calcd.$^{+}$	Calcd. from Eq.(8)	Calcd. Eq.(7)	
$NiCl_2 \cdot 6H_2O$	2103.3	2067.6	344.3	333.3	3099.1	3113.3	101.7
$NiCl_2 \cdot 4H_2O$	1516.7	1480.2	242.7	254.7	2996.2	3006.2	105.0
$NiCl_2 \cdot 2H_2O$	922.2	892.8	175.7	176.1	2885.3	2890.3	110.5
$NiCl_2 \cdot H_2O$	–	599.1	–	136.8	2807.5	–	–
$NiCl_2$	305.4	–	97.5	–	2752.2	–	–

*Calculated from Eq (5)

$^{+}$Calculated from relation $-[S^{\circ}_{f,m} - S^{\circ}_{f,n}] = (n-m)\ 44$ J·mol^{-1}·K^{-1}

$NiCl_2$ as reported in literature [18] are given in Table 7 from which it can be seen that the difference of heat of formation of two adjacent hydrates follow closely the following empirical relationship [19]

$$\Delta H^{\circ}_{f,m(c)} - \Delta H^{\circ}_{f,n(c)} = (n - m)\ 239.7\,kJ\cdot mol^{-1} \quad (5)$$

The hydration of anhydrous $NiCl_2$ may be written as

$$NiCl_2\ (c) + nH_2O\ (l) \rightarrow NiCl_2\cdot nH_2O\ (c)$$

Equation (5) enables us to estimate heat of hydration of the anhydrous salt (ΔHw) using the following relationship

$$\Delta Hw = \Delta H^{\circ}_{f,n(c)} - \Delta H^{\circ}_{f,o(c)} - n(\Delta H^{\circ}_{f,H_2O(g)} + L_{H_2O}) \quad (6)$$

where $\Delta H^{\circ}_{f,H_2O(g)}$ = heat of formation of gaseous water at 298 K

L_{H_2O} = latent heat of evaporation of water at 298 K.

ΔHw is related to lattice energy values of the crystalline salts by the following relationship

$$\Delta Hw = U_{l(n)} - U_{l(o)} + nRT - n\,L_{H_2O} \quad (7)$$

where $U_{l\,(n)}$ = lattice energy of $NiCl_2\cdot nH_2O$

$U_{l(o)}$ = lattice energy of anhydrous chloride.

Knowing the difference of $\Delta H^{\circ}_{f,n(c)} - \Delta H^{\circ}_{f,o(c)}$ from the empirical equation (5) and the literature [20] values of $U_{l(o)}$, L_{H_2O} and $\Delta H^{\circ}_{f,H_2O(g)}$ lattice energies of the different hydrates of $NiCl_2$ can be easily calculated at 298 K.

Lattice energy values of hydrated chlorides have also been estimated directly from Born-Haber cycle using the literature data of the heats of formation of different crystalline salts. The equation used is as follows:

$$-U_{l(n)} = S_{Ni} + D_{Cl_2} + I_{Ni^{2+}} - 2E_{Cl^-} - \Delta H^{\circ}_{f,n(c)} + n\Delta H^{\circ}_{f,H_2O\,(g)} \quad (8)$$

where S_{Ni} = heat of sublimation of Ni at 298 K ($422\ kJ\cdot mol^{-1}$)

D_{Cl_2} = heat of dissociation of Cl_2 molecule ($242.67\ kJ\cdot mol^{-1}$)

$I_{Ni^{2+}}$ = successive ionization potential of Ni^{2+} (27.5 eV)

E_{Cl^-} = electron affinity of Cl (3.61 eV)

and 1 eV = 96.44 kJ

The values obtained by the two methods agree well as can be seen from Table 7. Attempts were also made to calculate lattice energy values from electrostatic model of Kapustiniski [20]. The values obtained were however very low due to uncertainty in the interionic distance ($r_{cation} + r_{anion}$) and the extent of polarization induced by water molecule on this distance.

The main purpose of the above exercise is to check the validity of the literature value of heats of formation of different hydrates of $NiCl_2$ vis-à-vis empirical relationships of Grindstaff and Fogel. Since the enthalpy change of the formation of two consecutive hydrates in terms of per mol of water is nearly constant, entropy changes of the formation of hydrates may possibly serve as better criterion of their stability. Grindstaff and Fogel have also suggested that for most of the hydrated chlorides of divalent metal, the addition of each mol of water brings about an average entropy change of about 44 $J \cdot mol^{-1} \cdot K^{-1}$. However, for $NiCl_2$ hydrates deviation as high as ± 20 $J \cdot mol^{-1} \cdot K^{-1}$ is obtained from the literature value. It is therefore recommended that an entropy change value of 39.3 $J \cdot mol^{-1} \cdot K^{-1}$ would be a more suitable average value as suggested by Latimer [21].

Entropy of formation data indicate that there is a major structural change from tetrahydrate which has a stable structure. It is therefore not unusual that XRD indicates the presence of dihydrate even for sample calcined at 500°C. This is because adsorption of moisture even during the experiment tends to form dihydrate.

* * *

The authors wish to express their sincere thanks to Mr. D. N. Dey, Head, Pyrometallurgy Division for his keen interest and constant support during the course of investigation. Thanks are also due to Director, Regional Research Laboratory, Bhubaneswar for his kind permission to publish this paper. One of the authors (S. K. M.) is thankful to the Council of Scientific and Industrial Research, New Delhi for awarding a Junior Research Fellowship.

References

1 M. L. Skow, R. C. Kirby and J. E. Conley, Rept. Invest. U. S. Bur. Mines, No 5271, 1956, p. 29.
2 U. Scheffer and K. H. Ulrich, Ger. Often., 2, 249, 302, (to Friedrich Krupp G. m. b. h.)
3 K. N. Han and D. W. Fuerstenau, Mineral Processing Technol. Rev., 1 (1983) 1.
4 P. E. Queneau and H. J. Roorda, Min. Eng., 23 (1971) 70.
5 H. J. Roorda and P. E. Queneau, Trans. Inst. Min. Metall., 82c (1973) 79.
6 A. K. Saha, M. S. Mohanty, D. D. Akerkar and V. A. Altekar, A. T. B. Metall., 21 (1981) 129.
7 H. Jedlicka, Proc. Symp. Chloride Hydrometallurgy, Brussels 1977, p. 182.
8 H. N. Sinha and J. R. Tuffley, Extractive Metallurgy '81, The Inst. Mining, Metallurgy, London 1981, p. 421.
9 A. Van Petegham, U. S. Pat 4, 026, 773, 1977, (to Metallurgie Hoboken Oberpelt).
10 H. J. Borchardt and F. Daniels, J. Phys. Chem., 61 (1957) 917.
11 M. C. Ball and R. F. M. Coultard, J. Chem. Soc. A, (1968) 1417.
12 P. Lumme and K. Junnkkarinen Soumen Stihehti B, 41 (1968) 149, 220 and 261; 42 (1969) 306.
13 C. G. T. Guarini and R. Spinicia, J. Thermal Anal., 4 (1972) 435.
14 J. R. Willams and W. W. Wendlandt, Thermochim. Acta, 7 (1973) 275.
15 H. Tanaka and K. Maeda, Thermochim. Acta, 51 (1981) 97.
16 J. Ribas, A. Escuer, M. Serra and R. Vicente, Thermochim. Acta, 102 (1986) 125.

17 Y. Kirsch, S. Yariv and C. Shovel, J. Thermal Anal., 32 (1987) 393.
18 J. H. Dean (Ed.), Lange's Handbook of Chemistry, 13the Edn., McGraw Hill Book Co., New York Table 9–1.
19 M. F. C. Ladd and W. H. Lee, W. Reiss (Ed.) Progress in Solid State Chemistry, Vol. 1, Mc Millen Co. New York, 1964, p. 3.
20 W. M. Latimer, Oxidation Potentials, 2nd Edn., Prentice-Hall, New Jersey 1952, p. 359.

Zusammenfassung — Mittels isothermen und nichtisothermen (TG und DTA) Methoden wurden die Dehydratations- und die Zersetzungseigenschaften von ungetrockneten und teilweise getrockneten Proben von $NiCl_2 \cdot xH_2O$ sowohl in statischer Luftatmosphäre als auch in dynamischer Stickstoffatmosphäre untersucht. Während die isothermen Massenverlustsmethoden für die Unterscheidung der verschiedenen Reaktionsschritte ungeeignet sind, zeigen TG-Kurven bis 800°C nicht weniger als 5 Schritte in statischer Luftatmosphäre und vier Schritte in Stickstoffatmosphäre. Beide Methoden zeigen, daß $NiCl_2$ bis 400°C stabil ist, darüber findet in Gegenwart von Wasserdampf eine Dehydrochlorierung statt. Mittels Elementaranalyse, Röntgendiffraktion, IR- und Remissionsspektroskopie wurden die Zwischenprodukte von Dehydratation und Zersetzung bei verschiedenen Temperaturen charakterisiert. All dieser Methoden zeigen die Gegenwart von Wasser in den bei 400°–600°C kalzinierten Proben. Im Hinblick auf die möglichen strukturellen Veränderungen in den teilweise dehydratierten Produkten wurden thermodynamische Funktionen für verschiedene Schritte der Dehydratation berechnet und diskutiert.